IJCTA, 10(07), 2017, pp. 121-132

Iterative Decoding of Differential Space-time Coded FEC-based Multiple Descriptions

Saikat Majumder* and Shrish Verma*

Abstract : Differential space-time block codes (DSTBC) has been shown to be a recursive code and can be decoded using iterative techniques. In this paper we propose a three stage iterative decoding technique for differential space time coded FEC based multiple descriptions, in which DSTBC act as innermost code. FEC based multiple description system consisting of Reed-Solomon and convolutional code in 2D structure act as outer code in the proposed scheme. All the three stages iteratively exchange information and redundancy available at one stage of code improves the decoding performance of the composite system. We show that in the proposed scheme, because of three stage iterative decoding, significant improvement in PSNR is obtained for decoded multiple description image..
Keywords : Iterative decoding, space-time code, Reed-Solomon code, DSTBC, MIMO, multiple description coding.

1. INTRODUCTION

The growing demand for multimedia services on portable wireless devices has motivated researchers to explore more robust techniques for transmission of data. Multiple description (MD) coding is one of such techniques which have been proven to be effective on packet loss channels. MD coding generates multiple correlated descriptions of an image or video. Any combination of the available descriptions can be used to reconstruct the original source with certain fidelity, with increasing number of descriptions enhancing the quality of reconstruction. Thus due to individually decodable nature of the descriptions, the loss of some descriptions or packets does not jeopardize the reconstruction from the received packets. Multiple description coding techniques can be categorized into two major classes: source coder based and channel coder based techniques. From source coding perspective, some of the important techniques are MD scalar quantizer [1], MD correlating transforms [2]. It is the channel coding perspective, known as forward error correction (FEC) based multiple description coding, on which we shall concentrate in this paper.

FEC based multiple description coding has received more attention [3]-[9] in research literature compared to source-coder-based approach since it is flexible in generating arbitrary number of descriptions from progressive bitstream. Initially FEC based multiple description coding was proposed for packet loss channels. Mohr *et al*. [3] proposed a multiple description coding scheme which uses two dimensional (2D) arrangement of Reed-Solomon erasure correction codes for transmission of progressive images over packet loss networks. For graceful degradation of received image with packet losses, authors proposed construction of a balanced MDC from a progressive stream using priority encoding transmission (PET). In this scheme, contiguous symbols from the progressive stream are distributed across multiple descriptions, such that loss of some of the data packets do not affect the reconstructed image quality significantly. The source symbols are protected against loss of descriptions by using systematic Reed Solomon codes, and

* Department of Electronics and Telecommunication National Institute of Technology Raipur, India. *E-mail : smajumder.etc@nitrr.ac.in, shrishverma@nitrr.ac.in*

the level of erasure protection depends on the relative importance of the information symbols. This and similar works were extended to wireless channel (in contrast to packet loss or 'on-off' channel) by Sachs *et al*. [4] where convolutional code is used to provide additional protection to each description. In [10], a trellis based optimum redundancy allocation for n-channel FEC and using turbo code as channel code was proposed. In [5], 2D multiple description coding is employed with orthogonal frequency division multiplexing (OFDM) for transmission of progressive image, employing time and frequency diversity simultaneously. In all the above mentioned work, no feedback information is passed from FEC (*i.e*.Reed Solomon code) to channel code (*i.e*. convolutional code). In [6] an iterative algorithm is proposed for decoding of FEC based multiple descriptions codes, where correctly decoded Reed-Solomon code is used to enhance the error correction capability of convolutional code in next iteration. The iterative decoding is performed by passing only hard decisions between the decoders. Most of the above mentioned research concerning FEC-based multiple description coding, one typically applies channel soft-decision values to Viterbi algorithm as inner decoder. Hard decision output of channel decoder is then applied to a typical hard decision input Reed-Solomon decoder, *e.g*. Berlekamp-Massey algorithm [11]. It has been demonstrated in [8] that iterative soft-input soft-output decoding of concatenated Reed-Solomon and convolutional code can significantly improve decoder performance.

In spite of MDC and product code used for transmission of multimedia information, channel capacity remains an unmovable barrier [12]. The need for higher data rates can no longer be supported by simply allocating wider frequency bands and thus other techniques of increasing channel capacity has been explored by the researchers. One promising technique is the use of multiple-input multiple-output (MIMO) antenna systems. MIMO antenna systems utilize spatial diversity to achieve gain in link quality and hence capacity. Coordinated use of multiple antenna to achieve spatial diversity has been proposed in the form of space-time codes [13], [14] and layered space-time codes [15]. Alamouti code [13] and similar space-time block codes are designed based on the principle of orthogonality. Because of this, such schemes are sensitive to channel errors and are more difficult to design for fast fading channels. Space-time block code demodulation requires perfect channel state information (CSI) in order to achieve full diversity [16]. Estimation of channel information can be avoided by differential space-time block coding (DSTBC), which is similar to differential phase shift keying (DPSK) used in single-input single-output (SISO) antenna systems. But this advantage comes at a cost. DSTBC receiver requires about 3 dB more power than coherent receiver to achieve same error rate. Even with this loss, DSTBC is very competitive for fast fading channels because of the difficulty of obtaining channel information reliably. In [16], [17], iterative decoding technique by serial concatenation of DSTBC and convolutional code is proposed for iterative noncoherent detection of differential space-time code.

In this paper, we extend the scheme of Chang *et al.* [6] to include MIMO antenna system to achieve diversity gain in fading channel. Our innovation lies in incorporating iterative decoding between FEC based multiple description decoder and MIMO demodulator. This results in two significant outcomes. First outcome is improved decoding performance compared to similar existing schemes in literature for coherent scenario. Secondly, for case without CSI, we significantly narrow down the 3 dB performance gap compared to coherent receivers. As MIMO demodulator, we consider soft-input soft-output MAP DSTBC decoder, which can exchange soft information with outer decoders consisting of MAP decoder for convolutional code and RS decoder. For evaluating the performance of the proposed system, we compare it with similar iterative decoder in literature. Simulations are performed for cases with and without channel state information (CSI) at the receiver.

The structure of the paper is as follows. In Section 2, we provide the technical preliminaries related to MDC and differential STBC. In Section 3, we provide the system model. Section 4 describes the proposed iterative decoding algorithm in detail. In Section 5, simulation results and discussion are provided, and we conclude this paper in Section 6.

2. PRELIMINARIES

A. FEC-Based Multiple Description Coding

Fig. 1 illustrates the actual realization of n-channel FEC based multiple description coding by applying unequal FEC to different parts of progressive bitstream. As seen in the figure, first source symbol (shown as 1) is encoded with (n, 1) RS code (column 1), source symbols 2 and 3 are encoded with (n, 2) RS code (column 2). Subsequent symbols are encoded in similar way with decreasing level of protection using (n, k_l) RS codes, where $k_1 \le k_2 \le \ldots k_1 \ldots \le k_L$, and L is the number of RS codewords. That is, the symbols in the beginning of the stream are given more erasure protection compared to the subsequent symbols in the stream because of relative importance of bits at the beginning of the progressive bitstream. Any error or erasures in *l-th* column (of RS code) can be corrected if k_l symbols are received correctly. Descriptions or packets are formed by taking symbols row by row from the RS codes as shown in the figure. In this process, the progressive data is converted into multiple descriptions in which contiguous information is spread across multiple packets. Similarly, if any q out of n descriptions (horizontal) are received without any error, those codewords (vertical) with source symbols less than or equal to q can be recovered. Recovery of q descriptions will result in source or image distortion of $D(R_q)$, where D(R) is distortion-rate function and R_q is the rate corresponding to information symbols of q descriptions. Descriptions thus formed are appended with CRC and channel coded with recursive systematic convolutional code (RSCC) before transmitting over wireless channel to the destination.

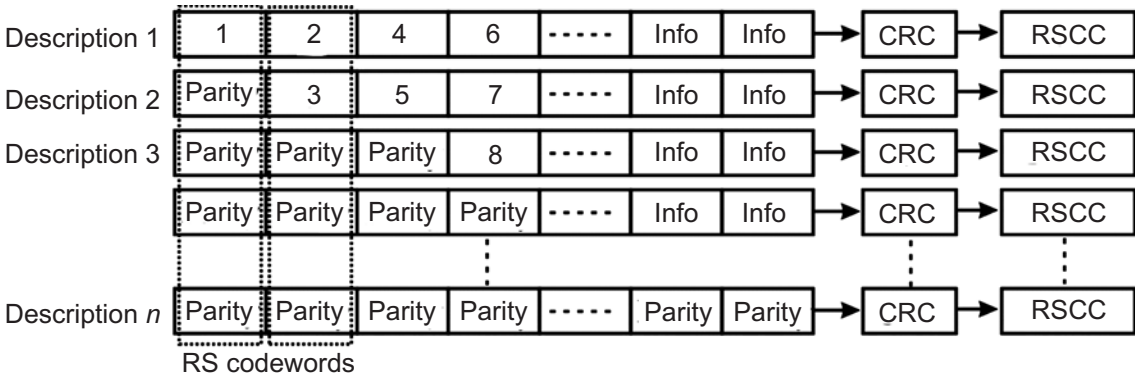

Figure 1: Formation of multiple descriptions from a progressive bitstream using Reed-Solomon code and convolutional code

B. Differential Space-Time Codes

In this paper we shall focus on differential space-time block code (DSTBC) of Hughes [21] for multiple antenna transmission. DSTBC can be demodulated without channel knowledge at a loss of 3 dB in signal-to-noise ratio (SNR) with respect to decoding similar space time code with complete channel knowledge. DSTBC code of Hughes is based on unitary matrices with a group structure, forming a space-time group code. If G be the group of unitary matrices, then $G^H G = GG^H = I$ for all $G \in G$. For a system of T transmit antennas with constellation C, for space time code $C \in C$ and for any $S \ge T$ there is a matrix D such that $C = DG$ for all $G \in G$ [12]. For example, with $T = S = 2$, the BPSK group is $G = \{G^{(0)}, G^{(1)}, G^{(2)}, G^{(3)}\}$, where

$$G^{(0)} = \begin{bmatrix} 1 & 0 \\ 0 & 1 \end{bmatrix} = -G^{(1)}$$

$$G^{(2)} = \begin{bmatrix} 0 & 1 \\ -1 & 0 \end{bmatrix} = G^{(3)} \quad (1)$$

and

$$D = \begin{bmatrix} 1 & -1 \\ 0 & 1 \end{bmatrix} \quad (2)$$

Encoded output in DSTBC, similar to differential phase shift keying, depends on the previous transmitted symbol. The fundamental difference equation for the calculation of encoded symbol at time i is

$$X_i = C_i = G^{(f(d_i))} C_{i-1} \tag{3}$$

For calculating first symbol C_1 (at time $i = 1$), the reference symbol taken is $C_0 = D$. In (3), $G^{(f(d_i))}$ is one of the symbols in the group G and $f(d_i)$ is a rule or function that maps bits pairs $d_i \in \{00,01,10,11\}$ to one of the four symbols in the set G. Group property ensures that C_i is a codeword if $C_{i-1} \in C$ is a codeword. X_i is used to indicate the transmitted DSTBC symbol. The S rows of C_i are transmitted as S consecutive space-time symbols. To decode the received signal y_i, there is a simple differential receiver which computes [21]

$$\hat{G} = \max_{G \in G} P \mathbb{R} \operatorname{Tr} G y_i y_{i-1} \tag{4}$$

In contrast to straight forward method of decoding given in (4), which incurs a 3 dB loss, we shall apply MAP decoder proposed in [16] for iterative decoding. Because of one unit delay involved in differential operation in (3), the encoder can be described by a trellis similar to convolutional code. Hence, MAP decoding by algorithms like BCJR [22] is also possible.

3. SYSTEM DESCRIPTION

The basic transmitter is shown in Fig. 2. Multimedia information is encoded by a progressive source encoder (*e.g.* SPHIT or JPEG 2000) to produce a bitstream u. The contiguous source bits are grouped into RS code symbols of m bits, *i.e.* $\in GF(2_m)$. As described in Section 2, these symbols are encoded with (n, k) RS code with level of protection depending on relative importance of information symbols. If the RS codewords are arranged as columns in Fig. 1, descriptions or packets are obtained by extracting symbols along the rows. Each descriptions is encoded, row-by-row, using recursive systematic convolutional code (RSCC) to produce bitstream r. Bits in a RSCC coded description are interleaved and fed into DSTBC encoder block for transmission through wireless channel.

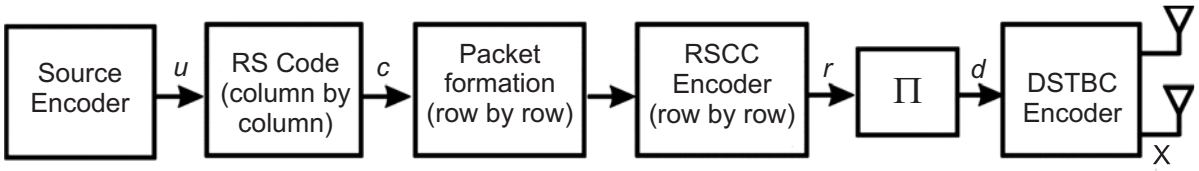

Figure 2: Encoder block diagram consisting of cascade of FEC based multiple description coder and DSTBC

Transmission takes place over a channel with T transmit and U receive antennas. At time slot i, the transmitting antennas transmits S rows of STBC symbol X_i over the channel. The demodulated baseband signal at a receive antenna at time i is

$$y_i = \sqrt{\frac{\rho}{T}} X_i H_i + N_i \tag{5}$$

where $H_i = [h_{tu}(i)]$ is the T × U channel gain matrix, N_i is AWGN matrix with variance of each element being $\sigma^2 = N_0/2$, and X_i is transmitted code from (3). At the receiver we propose three stage serially concatenated iterative decoding scheme where information is exchanged to and fro between DSTBC demodulator (inner decoder), RSCC decoder (middle decoder) and RS decoder (outer decoder). The serially concatenated decoder is shown in Fig. 3. Inner and middle decoder use the a posteriori probability (APP) decoding algorithm, whereas outer decoder use the hard decision algebraic decoding algorithm by Berlekamp and Massey [23]. The three stages form two iterative decoding loops: inner decoding loop and outer decoding loop, as explained in next section.

4. THREE STAGE ITERATIVE DECODER

In the iterative decoder of Fig. 3, the inner decoding loop consists of DSTBC APP decoder and RSCC APP decoder. DSTBC decoder receives signal y_i at time i and outputs extrinsic information $L^e(d_i)$, which is then deinterleaved and applied to RSCC APP decoder as a priori input $L^a(r_i)$. Extrinsic output $L^e(r_i)$ is applied back to DSTBC APP decoder, while a posteriori output $L^p(r_i)$ acts as input for outer loop. Both the decoders in inner loop use BCJR algorithm for soft-input soft-output decoding. Outer decoding loop consists of performing hard decision on output $L^p(r_i)$ of RSCC decoder and hard decision RS decoding by Berlekamp-Massey algorithm. RS code being block code, it is not difficult to identify those RS codewords (columns in Fig. 1) which were decoded successfully. Column indices $I = \{i_1, i_2, ...\}$ of the successfully decoded RS code is passed to the soft value modification block, which modifies the a priori input to RSCC APP decoder. Both the decoding loops are run for predefined number of iterations. In this paper, number of inner and outer iterations are indicated by L_I and L_O, respectively. Next we explain each of these blocks in more detail.

A. Inner Decoder: Decoding with CSI

To keep the calculations simple, we consider a system with two transmit and one receive antenna as described in Section 2. Generalization to multiple transmit and receive antennas is straight forward. At time i, if $X_i = C_i$ were transmitted, (5) can be written as

$$y_i = \sqrt{\frac{\rho}{T}} C_i H_i + N_i \tag{6}$$

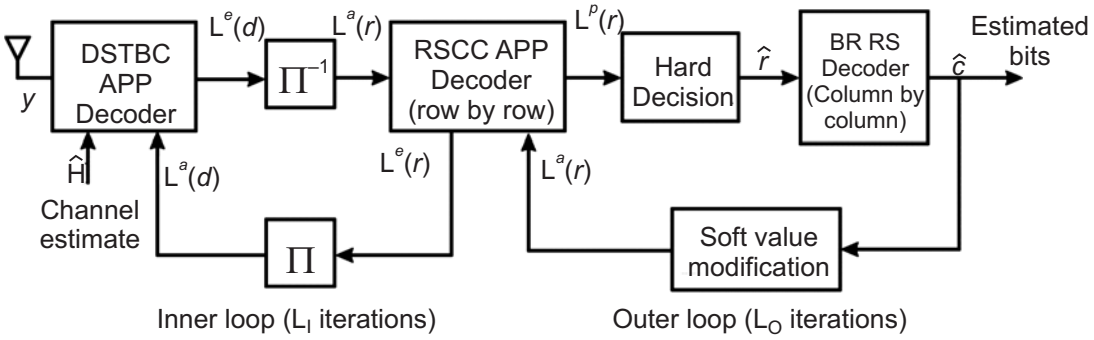

Figure 3: Iterative decoding of FEC based multiple descriptions, consists of three concatenated stages

where $y_i = [y_{1i}, y_{2i}]^T$ is a vector of two discrete received signals. Received signal probability conditioned on transmitted code and channel gain is then

$$p(yi \mid C_i, H_i) \propto \exp\left(-\frac{1}{2\sigma^2} || Y_i - C_i H_i ||^2\right) \tag{7}$$

The APP decoder utilizes the conditional probability in (7) for optimal decoding. The decoder calculates APP or log-likelihood ratio (LLR) of each bit

$$L^p(d_{ji}) = \log \frac{P(d_{ji} = 1|Y)}{P(d_{ji} = 0|Y)} \tag{8}$$

where d_{ji} is the j-th bit of the i-th transmitted DSTBC symbol and $Y = [y_1, \ldots, y_i, \ldots]$ is the entire received sequence. In our special case, $j = 1, 2$ indicates two bits in each symbol.

As mentioned earlier, DSTBC encoding can be represented with a trellis and can be decoded with usual trellis based decoding methods like Viterbi and BCJR decoder. Trellis diagram for code set defined by (1) and (3) is shown in Fig. 4(a), where state of the encoder $S_i = C_i$ are transmitted DSTBC code itself. There are M transitions per state, where $M = |G|$ is the cardinality of set G. Because of optimal and SISO nature of BCJR algorithm, it is used here for APP decoding of DSTBC. The set of all state transitions (m', m) corresponding to input bit $d_{ji} = b$ be is defined by the trellis in Fig. 4(a), where

$$\{(m', m) : d_{ji} = b, S_{i-1} = m', S_i = m\} \quad (9)$$

These are the set of transition at time i corresponding to input G_i, where $G_i = f(d_i)$ has been obtained by simple mapping from a pair of bits. Probability of transition from state m' to m at time i is

$$\sigma_i(m', m) = P(S_{i-1} = m', S_i = m, Y) \quad (10)$$

and can be written in terms of BCJR algorithm as

$$\sigma_i(m', m) = \alpha_{i-1}(m') \gamma_i(m', m) \beta_i(m) \quad (11)$$

where $\alpha_i(m) = \sum_{m'} \alpha_{i-1}(m') \gamma_i(m', m)$ is obtained through forward recursion through trellis and $\beta_i(m) = \sum_{m'} \beta_{i+1}(m') \gamma_{i+1}(m, m)$ is obtained by backward recursion. Using (7), the transition metric between state m' and m is given as

$$\gamma_i(m', m) = P(G_i) p(y_i \mid C_i H_i) \approx \exp\left\{\sum_j d_{ji} L(d_{ji}) - \frac{}{} || Y_i - C_i H_i ||\right\} \quad (12)$$

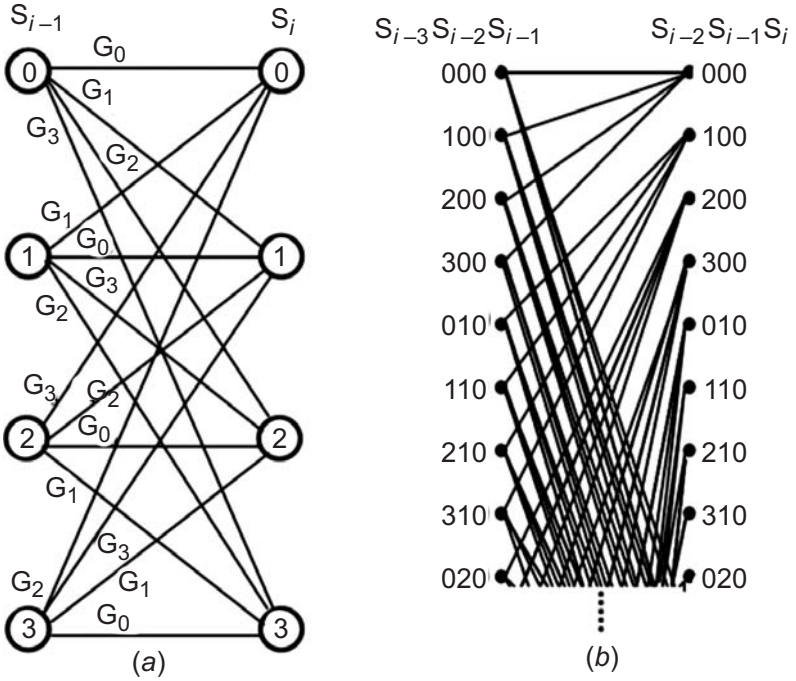

Figure 4: (*a*) Basic trellis structure of BPSK group DSTBC, (*b*) Section of extended trellis of BPSK group DSTBC for P = 2 having 64 states

where, $L^a(d_{ji})$ is *a priori* LLR obtained from the middle decoder. APP LLR for each bit is then calculated as

$$L^p(d_{ji}) = \frac{\sum_{(m', m): d_{ji}=1} \sigma_i(m', m)}{\sum_{(m', m): d_{ji}=0} \sigma_i(m', m)} \quad (13)$$

The extrinsic LLR which is passed on to the next decoder is

$$L^e(d_{ji}) = L^p(d_{ji}) - L^a(d_{ji}) \quad (14)$$

B. Inner Decoder: Decoding with Estimated CSI

In (12), fading channel gain coefficients or CSI are required for calculation of transition metric between states. Similar to DPSK, channel state information is not essential for decoding DSTBC successfully. If current channel gain $\hat{H}_i$ is not known, they can be estimated using linear prediction [25] using previous channel estimates $\tilde{H}_i$.

$$\hat{H}_i = \sum_{m=1}^{p} w_n \tilde{H}_{i-n} = \frac{1}{2} \sum_{n=1}^{p} w_n C_{i-n}^{H} y_{i-n} \quad (15)$$

where, P is the prediction order and $w = [w_1, \ldots, w_P]^T$ are predictor coefficients obtained by solving Wiener-Hopf equation $Rw = r$. Specifically for the case of T = S = 2 and channel gain being constant for a minimum duration of a STBC symbol (or two bit periods), matrix R is given as

$$\begin{bmatrix} r_0 & r_2 & & r_{2(P-1)} \\ r_2 & r_0 & \cdots & r_{2(P-1)+2} \\ \vdots & & \ddots & \vdots \\ r_{2(P-1)} & r_{2(P-1)} & \cdots & r_0 \end{bmatrix} \tag{16}$$

and $r = [r_2, r_4, \ldots, r_{2P}]^T$. The coefficients r^n are autocorrelation coefficients of the channel process. For Rayleigh flat fading channels, the autocorrelation is $r_n = J_0 (2\pi f_D T_s n)$ with $r_0 = 1 + 2\sigma^2$, where f_D is maximum Doppler frequency and T_s is sampling period. J_0 is first order Bessel function.

Using the channel estimate in (15), Nguyen and Ingram [16] calculated the transition metric $\gamma_i (m', m)$ between states as

$$\exp\left\{\sum_j d_{ji} L^a(d_{ji}) - \frac{1}{2\sigma^2_{pre}} || y_i \frac{1}{2} \sum_{n=1}^{p} w_n C^H_{i-n} y_{i-n} ||^2\right\} \tag{17}$$

The variance term in (17) is $\sigma^2_{pre} = (1/2) r_0 \{1 - \sum_{n=1}^{p} w_n (r_{2n}/r_0)$. The symbols $C_{i-1}, \ldots, C_{i-P}$ are replaced according to per-survivor principle [26]. For this purpose, MAP BCJR algorithm is now carried over expanded trellis with M^P states and there are M transitions per state for input corresponding to $G \in G$. As an example, we show a section of trellis with M = 4, P = 2 or 64 states in Fig. 4(*b*). For P = 2, states are defined as combination of three possible states (from basic trellis) or DSTBC outputs $S_{i-2} S_{i-1} S_i = C_{i-2} C_{i-1} C_i$. If states $m' = S_{i-3} S_{i-2} S_{i-1}$ and $m = S_{i-2} S_{i-1} S_i$, the transition metric in (17) is calculated using the state $S_{i-2} S_{i-1} S_i = C_{i-2} C_{i-1} C_i$.

C. Middle RSCC APP Decoder

The inner decoder passes extrinsic information $L^e(d_{ji})$ to next stage, which on deinterleaving, acts as a priori information $L^a(r_i)$ for the RSCC APP decoder. The APP decoder for RSCC is conventional SISO BCJR decoder [22]. It calculates the a *posteriori* LLR of output as $L^p(r_i)$ and binary hard decision is performed on it

$$\hat{r_i} = L^p(r_i) - L^a(r_i) \tag{18}$$

where sgn is the signum function. The hard decision $\hat{r_i}$ passed on to outer RS decoder. The extrinsic information of the coded bits, which is returned back to inner decoder, is

$$L^e(r_i) = L^p(r_i) - L^a(r_i) \tag{19}$$

D. Outer RS Decoder

The outer decoder stage consists of CRC and RS decoder. CRC block is not shown in Fig. 2 and Fig. 3 to avoid cluttering the figures. CRC decoder detects whether each description contains bit errors. Descriptions having bit errors are declared as an erasure for RS decoding. As stated before, for RS codeword *l* having $n - k_l$ parity symbols, the RS decoder (*i.e.* Berlekamp-Massey algorithm) can correct up to $n - k_l$ erasures. Berlekamp-Massey algorithm is an well known algorithm for decoding RS codes and can correct both errors and erasures [11].

Since, $k_1 \le k_2 \le \ldots k_1 \ldots \le k_L$ due to unequal error protection, it is very likely that the correctly decoded RS codewords (columns in Fig. 1) would be placed contiguously at the left end of the product code. Let $I = \{i_1, i_2, \ldots\} \subseteq \{1, 2, \ldots, L\}$ be the set of column index which have been correctly decoded. If |I| is the cardinality of set I, we know that there are $m|I|$ correct bits in each description, where m is the number of bits per RS code symbol. These bits correspond to the $m|I|$ information bits of each convolutional code. The function

of soft value modification block in Fig. 3 is to modify the a priori LLR bits in $L^a(r_i)$ corresponding to these m|I| possibly correct bits in each description. We modify the bit LLRs corresponding to these symbols by setting the absolute LLR values to preset maximum, while their signs remain the same. For better explanation, soft value modification is shown in the form of pseudo code in Algorithm 1. This accelerates the convergence of the succeeding MAP decoding of RSCC code and offer better error performance.

Algorithm 1: Soft value modification

Definition :

$L^a(r)$: *A priori* LLR input.

λ_{max} : Maximum LLR magnitude.

***c*□ :** Matrix consisting of columns of decoded RS codewords.

1. Interleave the RS codewords $\hat{c}$ to get $\tilde{I} = \Pi(\hat{c})$, where $\tilde{I} = [I_1, I_2, ..., I_n]^T$. Rows of bits I_i is the systematic part of hard decision estimate of *i*-th RSCC codeword.
2. For each row $i \in [1, n]$ and column $j \in [1, p]$, do
   - if $(F_{RSCC}(i) = 0)$ and $(F_{RS}(j) = 1)$
   - For each bit $b \in [(j-1)m + 1, jm]$ in the selected RS symbol, set

$$L^a(r)(i, b) = \begin{cases} \lambda_{max}, & \text{if } I_i(b) = 0 \\ -\lambda_{max}, & \text{if } I_i(b) = 1 \end{cases}$$

   - Modified a priori input to middle decoder is $L^a(r)$.

5. SIMULATION RESULTS

In this section we evaluate the performance of the proposed iterative decoding algorithm. The standard 8-bits-per-pixel (bpp) 128 × 128 images are encoded using the well-known SPIHT algorithm [19] to produce a progressively coded bitstream of rate 2 bpp. The bitstream was converted to a stream of $GF(2^8)$ symbols, where each symbol was obtained by combining $m = 8$ bits. This serial symbol stream was converted into 128 parallel bitstreams or descriptions using FEC-based multiple description encoder algorithm by Mohr *et al.* [3]. Mohr's algorithm provides the values of k_i for the RS codes using a hill climbing optimization approach. The multiple description encoder uses (n, k_i) RS code, where $n = 128$ and the description size is 32 RS code symbols (*i.e.* L = 32). All the descriptions are CRC coded. RSCC of rate 1/2 and generator polynomial (15, 17)8 is applied for channel coding. While decoding, it is assumed that any error in a description is detected by CRC and the description will be treated as erasure.

The goal of our simulation is to see how the proposed receiver with RS-RSCC-DSTBC iterative decoding compares with reference MDC iterative decoder proposed in literature. For comparison we consider baseline scheme proposed in [6] consisting of RS-RSCC iterative decoder. For fair comparison, we encode the RSCC coded descriptions in baseline scheme with Alamouti STBC [13]. We evaluate the performance in terms of peak-signal-to-noise ratio (PSNR) as function of average channel SNR. PSNR is calculated from expected distortion E(D) as $PSNR = 10 \log(255^2/E(D))$. In all results, we shall compare the channel SNR required to achieve maximum PSNR, unless mentioned otherwise. There are two set of computer simulation results.

In the first set of simulations, we study the effect of iteration on the improvement in PSNR curve when CSI available at the receiver. For this purpose the proposed scheme is tested over Rayleigh fast fading channel, *i.e.* fading coefficients are assumed to be constant for at least the duration of STBC symbol. Fig. 5 shows improvement in PSNR curve with number of iterations. The iterations are 'global' in the sense that one iteration of inner loop is followed by one iteration of outer loop and so on. For clarity, one such global iteration is indicated in figure as $(L_I, L_O) = 1$. With two iterations (indicated as $(LI, L_O) = 2$ in the figure), the transmission power required to achieve maximum value of PSNR is about 1.5 dB less compared to PSNR for one iteration $(L_I, L_O) = 1$. Maximum value of PSNR is obtained for four iterations $(L_I, L_O) = 4$ and

channel SNR of 1.4 dB. It can also be observed that rate of improvement of PSNR as function of channel SNR (as indicated by the slope of curve) improves with number of iterations. This may be attributed to the acceleration of convergence provided by 'turbo-like' iteration decoding architecture.

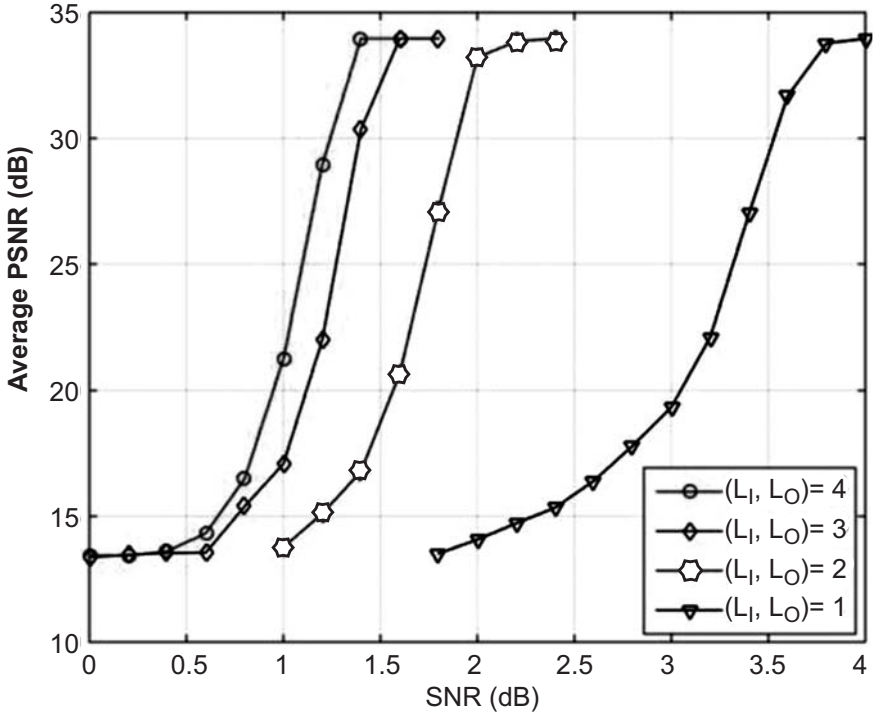

Figure 5: PSNR as function of channel SNR for different number of global iterations in Rayleigh fading channel

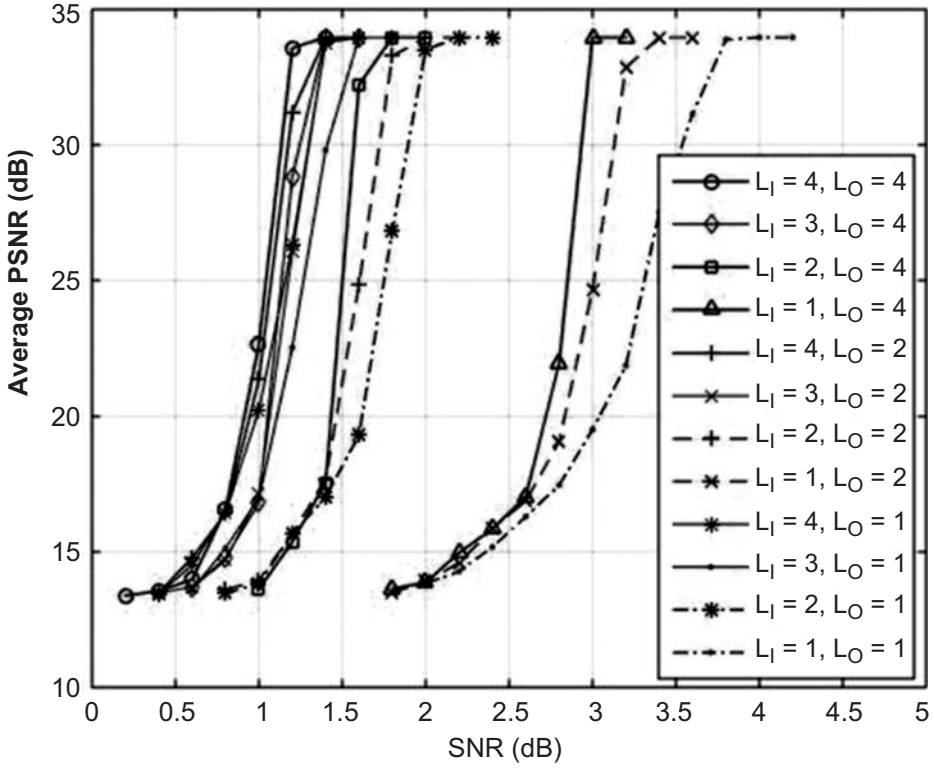

Figure 6: PSNR as function of channel SNR for different values of inner and outer loop iterations in Rayleigh fading channel

Next set of simulations were performed for 'local' iterations : L_I number of iterations of inner loop is followed by L_O number of iteration of outer loop. This allows us to isolate the decoding gain provided by the individual decoding loops. As shown in Fig. 6, keeping number of outer iterations L_O to a constant value, number of inner iterations L_I are varied from one to four. For four number of inner iterations

followed by four outer iterations (*i.e.* (L_I, L_O) = 4, maximum PSNR is obtained at channel SNR of 1.4 dB, which is 1.6 dB less power compared to (L_I = 1, L_O = 4). Also, the gain provided by outer loop iterations varies as function of L_I. For instance, if L_I = 1, the gain provided by four iterations of outer decoding loop is 0.8 dB in terms of channel SNR. This value reduces to 0.2 dB of channel SNR when L_I = 4. This can be interpreted as follows. If code redundancy is not completely exploited by the inner decoding loop, it can be utilized to a certain extent in the outer decoding loop. Since, outer decoding loop utilizes hard decisions for iteration gain, it does not provide gains comparable to a soft decision iterative decoder similar to inner loop.

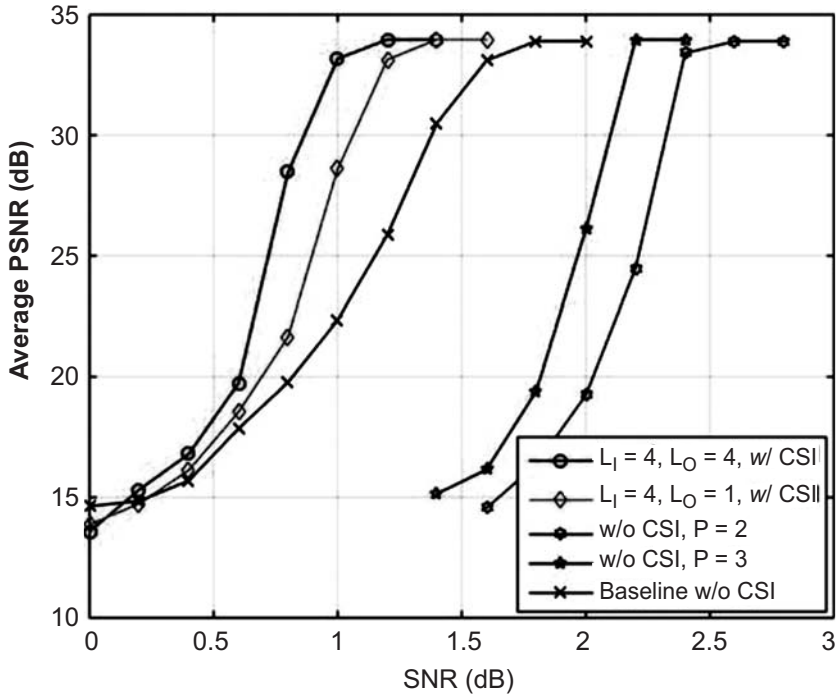

Figure 7: PSNR performance of proposed scheme compared to baseline scheme as function of channel SNR in Jake's channel with $f_D T_s$ = 0.01

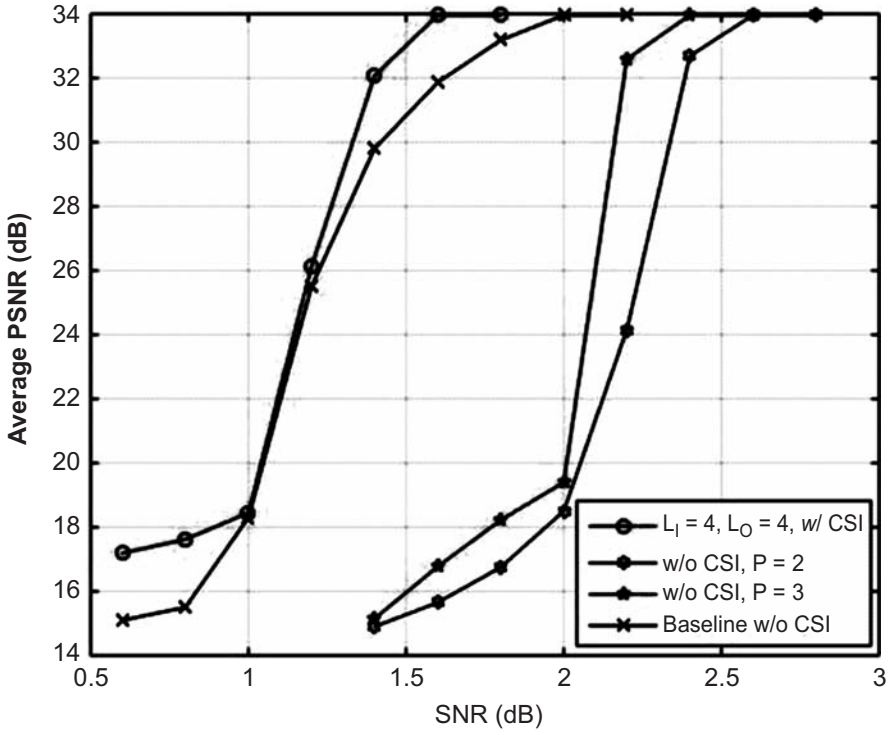

Figure 8: PSNR performance of proposed and baseline scheme in Jake's channel with $f_D T_s$ = 0.005

Second set of simulations are performed for Jake's fading model. The proposed scheme, with and without CSI, is compared to the baseline scheme (with CSI). Fig. 7 shows the simulation result for high mobility channel in which $f_D T_s = 0.01$. If CSI is available at the receiver, the proposed scheme achieves maximum PSNR at channel SNR of 1.2 dB, whereas this value is 1.8 dB for baseline scheme. Thus, the proposed scheme achieves the same PSNR performance for 0.6 dB less power. When using linear prediction and per-survivor processing for non-coherent case, the difference in channel SNR (to achieve maximum PSNR) compared to coherent case is 1.0 dB and 1.4 dB for prediction order of 3 and 2, respectively. Thus, proposed iterative decoding scheme reduces the 3 dB performance gap of differential detection system to a value of 1.0 dB. With higher order of prediction P, this gap can be reduced further.

Fig. 8 considers lower mobility channel with $f_D T_s = 0.005$. Maximum PSNR is achieved at channel SNR of 1.6 dB for the proposed scheme, whereas baseline scheme requires channel SNR of 2.0 dB. Power required for baseline scheme is 0.4 dB higher compared to proposed scheme. With linear prediction and per-survivor processing, maximum PSNR is obtained at SNR of 2.4 dB and 2.6 dB for prediction order of 3 and 2, respectively. For P = 3, channel SNR gap compared to coherent case is 0.8 dB, in contrast to a gap of 1.0 dB in Jakes' model with $f_D T_s = 0.01$. Finally, PSNR performance of some of the common test image is compared with baseline scheme at different values of channel SNR in Table 1.

6. CONCLUSION

A three stage iterative decoding scheme consisting of DSTBC as inner code and FEC based multiple description system as outer code has been proposed. FEC based multiple description code in turn can be considered product code of RS code and RSCC. The inner decoding loop consists of DSTBC and RSCC decoder exchanging soft decisions, whereas, outer decoding loop consists of RSCC decoder and RS decoder exchanging binary information. This scheme has been proposed for transmission of progressively coded image through fading channel, whereas, DSTBC provides space-time diversity. Simulation has been performed for Jakes' fading channel and compared to similar multiple description coding schemes in literature. The proposed system with CSI has been shown to perform significantly better compared to baseline scheme. In conventional schemes, differential detection without CSI results in performance loss of at least 3 dB. However, using the proposed three stage iterative decoder, we reduce this performance gap to 0.8 dB, which can be reduced further with higher order prediction.

Table 1
Performance advantage of proposed scheme in Jakes' fading channel with $f_D T_s = 0.01$ with CSI

Image	*Reconstructed image PSNR (average dB)*				
	SNR →	*0.8 dB*	*1.0 dB*	*1.2 dB*	*1.4 dB*
Lena	Iterative	28.46	33.17	33.96	33.96
	Baseline	19.77	22.35	25.87	30.50
Baboon	Iterative	19.90	21.15	20.96	21.35
	Baseline	18.89	20.38	20.62	21.26
Cameraman	Iterative	26.88	26.66	26.76	27.06
	Baseline	24.94	25.36	25.93	27.05

7. REFERENCES

1. V. A. Vaishampayan, "Design of multiple description scalar quantizers," IEEE Transactions on Information Theory, vol. 39, no. 3, 1993.
2. Y. Wang, M. T. Orchard, and A. R. Reibman, "Multiple description image coding for noisy channels by pairing transform coefficients," IEEE First Workshop on Multimedia Signal Processing, pp. 419-424, 1997.
3. A. E. Mohr, E. A. Riskin, R. E. Ladner, "Unequal loss protection: graceful degradation of image quality over packet erasure channels through forward error correction," IEEE Journal on Selected Areas in Communications, vol.18, no.6, pp.819-828, June 2000.

4. D. G. Sachs, A. Raghavan, K. Ramchandran, "Wireless image transmission using multiple-description-based concatenated codes," Proc. SPIE 3974, Image and Video Communications and Processing, 300, April 19, 2000.
5. L. Toni, Y. S. Chan, P. C. Cosman, L. B. Milstein, "Channel Coding for Progressive Images in a 2-D Time-Frequency OFDM Block With Channel Estimation Errors," IEEE Transactions on Image Processing, vol.18, no.11, pp.2476-2490, Nov. 2009.
6. S.-H. Chang, P. C. Cosman, L. B. Milstein, "Iterative Channel Decoding of FEC-Based Multiple-Description Codes," IEEE Transactions on Image Processing, vol.21, no.3, pp.1138-1152, March 2012.
7. A. Bais, T. Dey, N. Sarshar, "Unequal channel protection of multiple description codes for wireless broadcast applications," Signal Processing: Image Communication, Volume 27, Issue 6, July 2012.
8. S. Majumder, S. Verma, "Iterative decoding of FEC based multiple description codes for image transmission over wireless channel," Twenty First National Conference on Communications (NCC-2015), pp.1-6, Feb. 27 - March 1, Mumbai, 2015.
9. S. Majumder, S. Verma. "Iterative Channel Decoding of FEC-Based Multiple Descriptions using LDPC-RS Product Codes," International Journal of Applied Engineering Research, vol. 11, no. 9, pp. 6160-6167, 2016.
10. N. Thomos, N. V. Boulgouris, M. G. Strintzis, "Optimized transmission of JPEG2000 streams over wireless channels," IEEE Transactions on Image Processing, vol.15, no.1, pp.54-67, Jan. 2006.
11. J-H. Jeng, T-K. Truong, "On decoding of both errors and erasures of a Reed-Solomon code using an inverse-free Berlekamp-Massey algorithm," IEEE Transactions on Communications, vol. 47, no. 10, pp. 1488-1494, Oct 1999.
12. C. Schlegel, A. Grant, "Differential space-time turbo codes," IEEE Transactions on Information Theory, vol. 49, no. 9, pp. 2298-2306, Sept. 2003.
13. S. M. Alamouti, "A simple transmit diversity technique for wireless communications," IEEE Journal on Selected Areas in Communications, vol. 16, no. 8, pp. 1451-1458, Oct 1998.
14. V. Tarokh, H. Jafarkhani, A. R. Calderbank, "Space-time block codes from orthogonal designs," IEEE Transactions on Information Theory, vol. 45, no. 5, pp. 1456-1467, Jul 1999.
15. G. J. Foschini, "Layered space-time architecture for wireless communication in a fading environment when using multi-element antennas," Bell labs technical journal 1.2, pp. 41-59, 1996.
16. A. V. Nguyen, M. A. Ingram, "Iterative demodulation and decoding of differential space-time block codes," 52nd Vehicular Technology Conference, 2000. IEEE-VTS Fall VTC 2000, pp. 2394-2400 vol.5, Boston, 2000.
17. Z. Jia, "Iterative noncoherent detection of coded differential space-time modulation in Rayleigh fading channels," IEEE 13th International Conference on Advanced Communication Technology (ICACT), pp. 1310-1315, 2011.
18. M. K. Howlader, Y. Yao, "Iterative decoding of serial concatenated differential space-time block coding under unknown fading channels," Proc. Wireless Communications and Networking Conference, WCNC 2008, 2008.
19. A. Said, W. A. Pearlman, "A new, fast, and efficient image codec based on set partitioning in hierarchical trees," IEEE Transactions on Circuits and Systems for Video Technology, vol. 6, no. 3, pp. 243-250, 1996.
20. H. Schwarz, D. Marpe, T. Wiegand, "Overview of the scalable video coding extension of the H. 264/AVC standard," IEEE Transactions on Circuits and Systems for Video Technology, vol. 17, no. 9, pp. 1103-1120, 2007.
21. B. L. Hughes, "Differential space-time modulation," IEEE Transactions on Information Theory, vol. 46, no. 7, pp. 2567-2578, Nov 2000.
22. L. Bahl, J. Cocke, F. Jelinek, J. Raviv, "Optimal decoding of linear codes for minimizing symbol error rate," IEEE Transactions on Information Theory, vol. 20, no. 2, pp. 284-287, Mar. 1974.
23. S. Lin and D. J. Costello, Error Control Coding: Fundamentals and Applications, 2nd ed. Prentice-Hall, Englewood Cliffs, NJ, 2004.
24. B. Liu et al., "LDPC-RS Product Codes for Digital Terrestrial Broadcasting Transmission System," IEEE Transactions on Broadcasting, vol.60, no.1, pp.38-49, March 2014.
25. J. Makhoul, "Linear prediction: A tutorial review," Proceedings of the IEEE, vol. 63, no. 4, pp. 561-580, 1975.
26. R. Raheli, A. Polydoros, C-K. Tzou, "Per-survivor processing," Digital Signal Processing, vol. 3, no. 3, pp. 175-187, 1993.